Available online at www.sciencedirect.com
ScienceDirect
Bioorganic & Medicinal Chemistry 16 (2008) 3959–3968
Bioorganic & Medicinal Chemistry

The structure-based design, synthesis and biological evaluation of DNA-binding bisintercalating bisanthrapyrazole anticancer compounds

Brian B. Hasinoff,[a,*] Hong Liang,[a] Xing Wu,[a] Lynn J. Guziec,[b] Frank S. Guziec, Jr.,[b] Kyle Marshall[b] and Jack C. Yalowich[c]

[a]*Faculty of Pharmacy, University of Manitoba, 50 Sifton Road, Winnipeg, MB, Canada R3T 2N2*
[b]*Department of Chemistry and Biochemistry, Southwestern University, Georgetown, TX 78628, USA*
[c]*Department of Pharmacology, University of Pittsburgh School of Medicine, Pittsburgh, PA 15261, USA*

Received 27 November 2007; revised 15 January 2008; accepted 17 January 2008
Available online 26 January 2008

Abstract—Anticancer drugs that bind to DNA and inhibit DNA-processing enzymes represent an important class of anticancer drugs. In order to find stronger DNA binding and more potent cytotoxic compounds, a series of ester-coupled bisanthrapyrazole derivatives of 7-chloro-2-[2-[(2-hydroxyethyl)methylamino]ethyl]anthra[1,9-**cd**]pyrazol-6(2H)-one (AP9) were designed and evaluated by molecular docking techniques. Because the anthrapyrazoles are unable to be reductively activated like doxorubicin and other anthracyclines, they should not be cardiotoxic like the anthracyclines. Based on the docking scores of a series of bisanthrapyrazoles with different numbers of methylene linkers (*n*) that were docked into an X-ray structure of double-stranded DNA, five bisanthrapyrazoles ($n = 1$–5) were selected for synthesis and physical and biological evaluation. The synthesized compounds were evaluated for DNA binding and bisintercalation by measuring the DNA melting temperature increase, for growth inhibitory effects on the human erythroleukemic K562 cell line, and for DNA topoisomerase IIα-mediated cleavage of DNA and inhibition of DNA topoisomerase IIα decatenation activities. The results suggest that the bisanthrapyrazoles with $n = 2$–5 formed bisintercalation complexes with DNA. In conclusion, a novel group of bisintercalating anthrapyrazole compounds have been designed, synthesized and biologically evaluated as possible anticancer agents.

1. Introduction

The clinical use of doxorubicin and the other anthracyclines is limited by the development of a cumulative dose-dependent and potentially fatal cardiotoxicity which is probably due to oxidative stress on the relatively unprotected cardiac muscle. Piroxantrone (DuP 942, CI 942, oxantrazole, or pirozantrone) and losoxantrone (DuP 941, CI 941, or biantrazole) are anthrapyrazole antitumor agents that were developed as non-cardiotoxic alternatives to the quinone-containing anthracyclines doxorubicin and daunorubicin.[1–3] These planar anthrapyrazoles intercalate into DNA[1,2] and promote DNA strand breaks.[3] We previously showed[4] in a structure-based 3D-QSAR study that a series of substituted anthrapyrazoles that we synthesized had potent cancer cell growth inhibitory effects.

Compounds with two DNA intercalating moieties and a suitable linker can potentially bind DNA much more strongly than a single intercalating group because of the favorable entropic advantage that ensues after the binding of the first intercalating group. DNA bisintercalating compounds, as exemplified by echinomycin, occur naturally and have progressed into clinical trials as antitumor agents.[5] Other purely synthetic bisintercalating compounds have been described in a recent review.[6] WP631 and WP762, which are bisintercalating bisanthracyclines that are based on daunorubicin with a xylenyl linker, have also been described.[7,8] These compounds bind DNA extremely strongly and inhibit cell growth at nanomolar concentrations. However, because WP631 and WP762 are anthraquinones they likely would be susceptible to reductive activation by a variety

Keywords: Bisanthrapyrazole; Bisintercalating; Anticancer; DNA-binding; Topoisomerase II; DNA; Molecular modeling; Docking; Cytotoxicity; K562 cells; Cardiotoxic.
* Corresponding author. Tel.: +1 204 474 8325; fax: +1 204 474 7617; e-mail: B_Hasinoff@UManitoba.ca

0968-0896/$ - see front matter © 2008 Elsevier Ltd. All rights reserved.
doi:10.1016/j.bmc.2008.01.033

of reducing enzymes to produce damaging reactive oxygen species, potentially leading to cardiotoxicity like daunorubicin and doxorubicin.[9] In this study we prepared a series of ester-coupled bisanthrapyrazoles based on **6**[4] (Fig. 1). In order to optimize binding to DNA and improve their growth inhibitory effects bisanthrapyrazoles with different numbers of methylene linkers were designed based on their ability to dock into an X-ray structure of double-stranded DNA. Compound **6** was chosen as the scaffold for the synthesis of a series of bisanthrapyrazole congeners because its side chain has a tertiary amine functionality (unlike piroxantrone, losoxantrone and other bisanthrapyrazoles synthesized[4]) that would be unreactive with the acid chlorides used to make the ester linkage. Compound **6** also contains an hydroxyl group at the end of the side chain which allows for esterification. Additionally, **6** had significant cell growth and topoisomerase IIα inhibitory activity.[4] In addition to measuring the cell growth inhibitory effects of the bisanthrapyrazoles we also measured their ability to bind to DNA, to inhibit topoisomerase IIα (EC 5.99.1.3), and to cause topoisomerase IIα-mediated DNA cleavage.

2. Results

2.1. Effect of the bisanthrapyrazoles on the thermal denaturation of DNA

Doxorubicin (2 μM), which is a well-known DNA intercalating drug, was used as a control and was observed to increase the ΔT_m of sonicated DNA by 13.2 °C from 71.0 °C. Under limiting conditions the value of ΔT_m is directly proportional to the logarithm of the equilibrium constant for ligand binding to DNA[10] and thus the value of ΔT_m was used directly in the free energy correlation analyses. Of the bisanthrapyrazoles studied **2** had the largest effect on ΔT_m, and thus bound the strongest to DNA (Table 1). Compounds **2** and **3** all bound to DNA in a stronger manner than the strongly binding DNA intercalator doxorubicin. Of the five bisanthrapyrazoles synthesized **1** bound to DNA was the weakest and increased ΔT_m about the same as the parent **6**. The other four bisanthrapyrazoles synthesized all bound more strongly than the parent **6**. The fact that **2**, **3**, and **4** all had ΔT_m values much greater than **6** suggests that these bisanthrapyrazoles may form bisintercalation complexes with DNA.

In a study[11] on the bisintercalator dye YOYO and its monomeric form YO-PRO it was shown that the slope of a plot of ΔT_m versus drug concentration is approximately twice that for the bisintercalator compared to the mono intercalator due to the bisintercalator occupying twice the number of intercalation sites on the DNA. The concentration dependence of ΔT_m for monomeric **6** (AP9) and the bisanthrapyrazoles **1**–**5** is shown in Figure 2A. The slopes ± SEM are plotted in Figure 2B. A comparison of the slopes by *t*-test showed that all bisanthrapyrazoles but compound **1** ($p > 0.5$, not significant) had slopes that were significantly different ($p < 0.001$) than monomer **6**. From the data in Figure 2A and a propagation of errors analysis compound **1** gave a ratio of the slopes of compound **1** to compound **6** of 1.0 ± 0.1 indicating mono intercalation. A similar calculation for compound **2** gave a ratio of slopes of 2.5 ± 0.2 which is in reasonable agreement with the theoretical value of 2. Similarly compounds **3**, **4**, and **5** give ratio of slopes of 2.0 ± 0.2, 1.5 ± 0.1, and 1.6 ± 0.2, respectively. These results suggest that all but **1** formed bisintercalation complexes with DNA. A ratio of slopes less than 2 for **4** and **5** may be due to these bisanthrapyrazoles forming mixed bis and mono intercalation complexes.

2.2. Effect of the bisanthrapyrazoles on cell growth inhibition

As shown in Table 1 all of the bisanthrapyrazoles inhibited the growth of K562 and K/VP.5 cells that had been continuously exposed to the drugs for 72 h. Compound **3** with 3 methylene linkers was the most potent of the compounds. These results suggest that the bisanthrapyrazoles were not too large or too charged to enter cells and the nucleus. In general, while all the bisanthrapyrazoles displayed low micromolar growth inhibitory effects, and were more potent than the parent **6**, there was not a large variation (3-fold) in IC_{50} values amongst the bisanthrapyrazoles.

2.3. The bisanthrapyrazoles inhibit the decatenation activity of topoisomerase IIα

As shown in Table 1 all of the bisanthrapyrazoles inhibited the decatenation activity of human topoisomerase IIα in the low micromolar concentration range, but only **4** achieved a potency nearly equal to that of the parent **6**. This assay is a measure of the ability of these compounds to inhibit the catalytic activity only, and was not a measure of whether these compounds acted as topoisomerase II poisons as do losoxantrone and piroxantrone[12,13] and some widely used anticancer drugs.[14,15]

2.4. Effect of bisanthrapyrazoles on the stabilization of the covalent topoisomerase IIα–DNA cleavable complex

Several widely used anticancer agents, including doxorubicin and the other anthracyclines, mitoxantrone and etoposide,[14,15] as well as losoxantrone and piroxantrone,[12,13] are thought to be cytotoxic by virtue of their ability to stabilize a covalent topoisomerase II–DNA intermediate (the cleavable complex) and act as topoisomerase II poisons. Topoisomerase II alters DNA topology by catalyzing the passing of an intact DNA double helix through a transient double-stranded break made in a second helix and is critical for relieving torsional stress that occurs during replication and transcription and for daughter strand separation during mitosis.[14,15] Thus, DNA cleavage assay experiments[16] as we previously described[4,17] were carried out using 100 μM etoposide as a positive control to see whether 50 μM of the test bisanthrapyrazoles stabilized the cleavable complex. As shown in Figure 3 the addition of etoposide (lane 8) to the reaction mixture containing topoisomerase IIα and supercoiled pBR322 DNA induced formation of linear pBR322 DNA. Linear DNA was identified by compar-

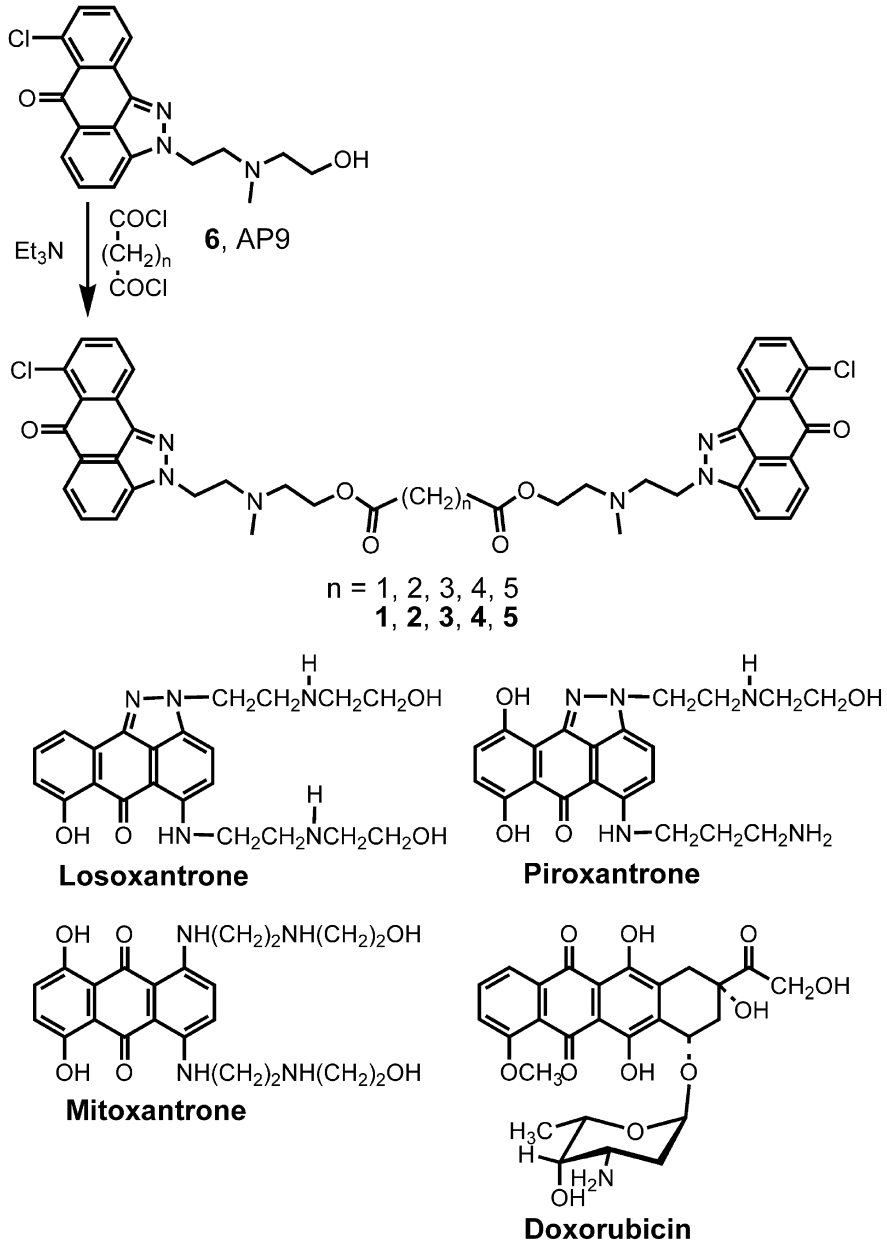

Figure 1. Reaction scheme and structures for the synthesis of the bisanthrapyrazoles **1**, **2**, **3**, **4**, and **5** (n = 1–5) prepared from **6** (AP9). Structures of losoxantrone, piroxantrone, mitoxantrone, and doxorubicin are also shown.

ison with linear pBR322 DNA produced by action of the restriction enzyme HindIII acting on a single site on pBR322 DNA (not shown). Although it may have appeared that the bisanthrapyrazoles were capable of inducing some linear DNA formation in the presence of topoisomerase IIα, the fluorescence of the bisanthrapyrazoles related to their binding to DNA made accurate determination of the amount of linear DNA problematic (Fig. 3). Similar problems were encountered with the anthrapyrazoles of our previous study.[4] As shown in lanes 5 and 7 both compounds **3** and **5** displayed significant fluorescence that interfered with quantitation of the linear DNA band. Based on integrated band intensities of linear DNA in Figure 3 none of the bisanthrapyrazoles appeared to induce formation of linear DNA comparable to that induced by etoposide (lane 8). However, given the problems in measuring the amount of linear DNA in these experiments, we cannot firmly conclude that the bisanthrapyrazoles do not poison topoisomerase II as we found with some of the anthrapyrazoles of our previous study.[4] The relaxed DNA band observed in lane 2 for the topoisomerase IIα control ran ahead of the supercoiled DNA in lane 1 (pBR322 control). Etoposide and all 5 bisanthrapyrazoles inhibited the relaxation of supercoiled pBR322 DNA of topoisomerase IIα, thus preventing the DNA band from migrating in a similar manner as in lane 2. Together these results indicated that etoposide inhibited topoisomerase IIα catalytic activity and induced DNA cleavage while the bisanthrapyrazoles acted primarily by inhibition of topoisomerase IIα strand passage reactions.

Table 1. DNA ΔT_m, cell growth inhibition and topoisomerase IIα inhibitory effects of the bisanthrapyrazoles

Compound	ΔT_m (°C)	MTS cell growth inhibition		Resistance factor[a]	Topoisomerase IIα inhibition
		K562 IC_{50} (μM)	K/VP.5 IC_{50} (μM)		IC_{50} (μM)
1	7.4	2.5	4.2	1.7	25
2	16.4	2.7	4.2	1.6	50
3	14.1	1.1	2.9	2.6	32
4	12.7	3.3	3.9	1.2	8.4
5	9.7	1.8	2.7	1.5	33
6[b], AP9	6.1	5.7	6.4	1.1	7.2
Losoxantrone[b]	18.1	0.12	0.22	1.8	7.3
Piroxantrone[b]	19.0	4.0	6.7	1.7	4.6
Mitoxantrone[b]	18.4	0.42	1.68	4.2	5.3
Doxorubicin[b]	13.2	0.08	0.41	5.1	ND

ND is not determined.

[a] The resistance factor was calculated from the ratio of the IC_{50} value for the K/VP.5 cell line divided by that for the K562 cell line.

[b] Data from reference.[4] Compound **6** (AP9) is the parent monomeric form of the bisanthrapyrazoles **1**, **2**, **3**, **4**, and **5** (n = 1–5).

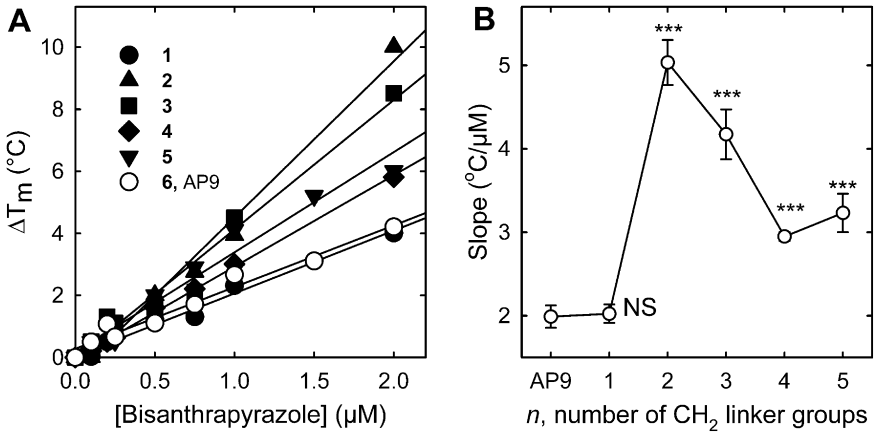

Figure 2. Concentration dependence of ΔT_m for the bisanthrapyrazoles binding to DNA. (A) Concentration dependence of ΔT_m for the bisanthrapyrazoles **1**, **2**, **3**, **4**, and **5** (n = 1–5) and parent monomer **6** for comparison. The solid straight lines are linear least squares fits to the data. (B) Concentration dependence of the slopes ± SEM calculated from the data in (A). Except for **1** (NS, not significant) the slopes of the plots in (A) for **2**, **3**, **4**, and **5** are all significantly (***$p < 0.001$) different than the parent **6**. Compounds with slopes approximately twice that of the parent monomer **6** indicate that they formed bisintercalation complexes with DNA.

2.5. The effects of the bisanthrapyrazoles on the growth of a K562 cell line compared to the K/VP.5 cell line with a decreased level of topoisomerase IIα

One method by which cancer cells increase their resistance to topoisomerase II poisons is by lowering their level or activity of topoisomerase II.[14,18] Cells containing less topoisomerase II produce fewer DNA strand breaks in the presence of topoisomerase II poisons and are less lethal to cells. These cell lines provide a convenient way to test whether a drug that inhibits topoisomerase II acts as a topoisomerase II poison.[19] Conversely, a lack of change in sensitivity of a putative topoisomerase II poison to a cell line with a lowered topoisomerase II level can be taken to indicate that poisoning of topoisomerase II is not an important mechanism for a particular agent. We previously reported that topoisomerase IIα and topoisomerase IIβ protein levels were reduced 6- and 3-fold, respectively, in the K/VP.5 cell line with acquired resistance to etoposide compared with K562 cells.[20,21] The IC_{50} for growth inhibition of K562 cells and K/VP.5 cells, measured as previously described[4] with the MTS assay, after a 72 h continuous treatment with a range of bisanthrapyrazole concentrations are compared in Table 1. Most of the bisanthrapyrazoles were slightly to moderately cross resistant (up to 2.6-fold for **3**), but none were as cross resistant as mitoxantrone or doxorubicin (4- to 5-fold). Thus, these results and the results of the cleavage assay (Fig. 3) offer only moderate support for the conclusion that the bisanthrapyrazoles inhibited cell growth by acting as topoisomerase II poisons.

2.6. Docking of the bisanthrapyrazoles into DNA

Compound **4** and bisanthrapyrazoles containing up to 9 methylene linkers (Fig. 1) all docked with their linkers located in the DNA minor groove. However, with the major groove not blocked **1**, **2**, and **3** docked with their linkers located in the DNA major groove with similar configurations, both with respect to the pyrazole rings and the amino side chains. For the bisanthrapyrazole **1** containing 1 methylene linker, only one of the bisanthrapyrazole rings was inserted into one of the intercalation sites, likely because the linker was too short

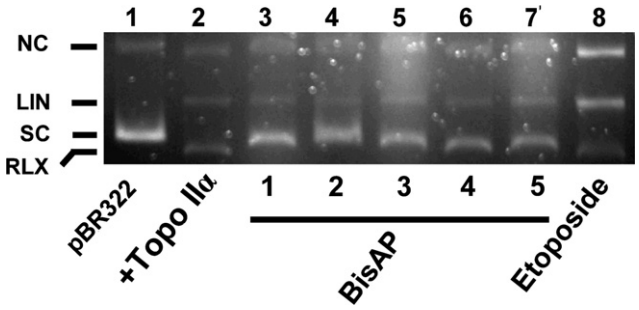

Figure 3. Effect of bisanthrapyrazoles **1**, **2**, **3**, **4**, and **5** on the topoisomerase IIα-mediated cleavage of supercoiled pBR322 DNA. This fluorescent image of the ethidium bromide-stained gel shows that topoisomerase IIα (Topo IIα) relaxed supercoiled pBR322 plasmid DNA (SC) to relaxed (RLX) DNA (lane 2, the band running slightly ahead of the SC band). pBR322 DNA in the absence of topoisomerase IIα is shown in lane 1. Topoisomerase IIα was present in the reaction mixture for all other lanes. As shown in lane 8 etoposide treatment (100 μM) produced linear DNA (LIN). A small amount of nicked circular (NC) is normally present in the pBR322 DNA. BisAP identifies the bisanthrapyrazoles **1**, **2**, **3**, **4**, and **5**. Based on densitometry, none of the bisanthrapyrazoles (50 μM) produced any significant amount of linear DNA above control levels (lane 2). Some of the fluorescent bisanthrapyrazoles present in the gel (lanes 3, 5, and 7) partially obscured the linear DNA band.

to allow for bisintercalation. However, all of the other anthrapyrazole rings of the other bisanthrapyrazoles docked were completely inserted into the two doxorubicin intercalation sites. The structure of **2** docked into DNA is shown in Figure 4.

The GOLDScores obtained when the major DNA groove was blocked for bisanthrapyrazoles ($n = 0$–9) are plotted as a function of n, the number of methylene linkers in Figure 5A. The bell-shaped plot shows a broad maximum with an n value in the 3–5 range suggesting that bisintercalation binding to DNA is predicted to be optimal in this range. The maximum value obtained from a quadratic fit (solid line) to the data indicated that an n value of 4.9 was optimal for binding to DNA.

The experimentally determined strength of binding to DNA determined using ΔT_m as a measure is shown plotted in Figure 5B as a function of n, the number of methylene linkers. The bisanthrapyrazole that experimentally bound the strongest to DNA was **2**, and this was followed closely by **3** and **4**. The maximum in the quadratic fit (solid line) for the data in Figure 5B for the bisanthrapyrazoles we synthesized ($n = 1$–5) indicated an n value of 3.0 was optimal for binding to DNA. Thus, the optimal number of methylene linkers calculated from the GOLD docking and the experimental number were in reasonably good agreement. These results suggest that docking of virtual bisanthrapyrazoles with varying linker lengths is a good way to select a range of optimal linker lengths prior to synthesis. This result shows that bisanthrapyrazole GOLD docking scores were a good predictor of optimal linker length for strength of binding to DNA. Also the GOLD docking scores were very good at predicting which bisintercalating compounds

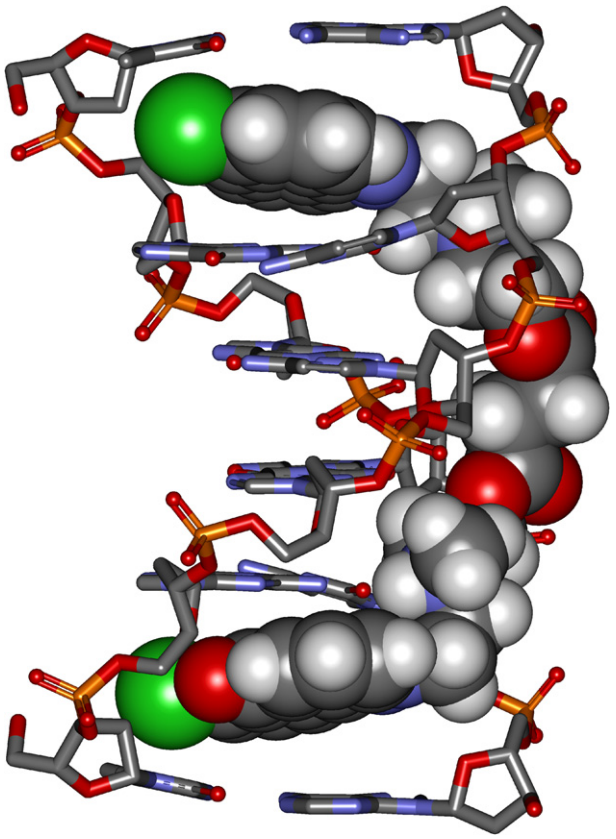

Figure 4. Docking of the protonated bisanthrapyrazole **2** into DNA. The highest scoring structure of the strongest DNA-binding bisanthrapyrazole **2** (CPK structure) is shown docked into DNA (stick structure). The H-atoms of the DNA are not shown for clarity. The DNA structure is 1DA9 from the Protein Data Bank and is a DNA–$(doxorubicin)_2$ X-ray structure in which two doxorubicin molecules are bound to a 6-base pair piece of DNA. Both doxorubicin molecules were removed and **2** was docked into one of the sites with the genetic algorithm docking program GOLD.

have too small a number of linker groups to achieve bisintercalation.

2.7. QSAR correlation analyses of GOLDScore, DNA-binding affinity, K562 cell growth inhibition, and topoisomerase IIα inhibition

A correlation analysis was carried out on the logarithm of the K562 IC_{50} values versus the GOLDScores and each of its component terms: DNA–ligand hydrogen-bond energy (external H-bond); DNA–ligand van der Waals (vdw) energy (external vdw); and the sum of the two ligand external terms as we previously described for a series of anthrapyrazoles.[4] No significant correlation was found (all p values greater than 0.1). Linear least squares regression analysis was also carried out on the ΔT_m values versus the GOLDScores. While ΔT_m was positively correlated with the GOLDScore (plot not shown) for the whole data set ($n = 1$–5) the correlation was not strong (r^2 of 0.1).

The logarithm of the K562 IC_{50} values versus ΔT_m was also not correlated (p of 0.9). In our previous study of a

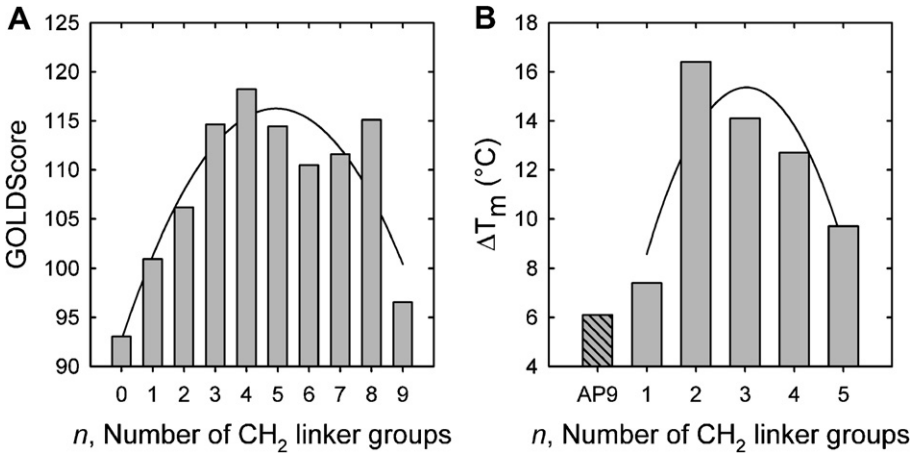

Figure 5. Calculated and experimental measures of binding of the bisanthrapyrazoles binding to DNA. (A) GOLDScores obtained from the docking of the bisanthrapyrazoles into DNA as a function of n, the number of CH_2 linker groups in the bisanthrapyrazoles. The solid line is a quadratic fit of the GOLDScore values for the bisanthrapyrazoles with $n = 0$–9. The maximum in the quadratic fit occurs at a value of $n = 4.9$. (B) Experimentally measured ΔT_m values for the bisanthrapyrazoles with $n = 1$–5 that were synthesized and parent **6** for comparison. The solid line is a quadratic fit of ΔT_m (solid line) for the bisanthrapyrazoles with $n = 0$–5. The maximum in the quadratic fit occurs at a value of $n = 3.0$.

series of anthrapyrazoles that we synthesized the logarithm of the K562 IC_{50} values and ΔT_m were highly correlated ($p = 4 \times 10^{-5}$).[4] Also similar to what we found for the anthrapyrazoles,[4] the logarithm of the K562 IC_{50} data was poorly correlated with the logarithm of the IC_{50} for the catalytic inhibition of topoisomerase IIα ($p = 0.4$). The lack of correlation with topoisomerase IIα activity IC_{50} does not necessarily indicate that these compounds lack activity as topoisomerase II poisons, but rather only that they did not act solely through their inhibition of the catalytic activity of topoisomerase IIα. Similarly, the logarithm of the IC_{50} for the catalytic inhibition of topoisomerase IIα was also poorly correlated (p of 0.7) with ΔT_m.

3. Discussion

In this study a series of bisanthrapyrazoles were designed using molecular modeling and docking into DNA in order to determine the optimal linker length for optimal binding to DNA and selection for their subsequent synthesis. An X-ray structure (1DA9)[22] of two molecules of doxorubicin separated by 4 base pairs bound to duplex DNA was used for the docking (Fig. 4). Five bisanthrapyrazoles based on **6** with 1–5 methylene linkers[4] were synthesized and chemically and biologically characterized. DNA melting temperatures ΔT_m (Table 1) were determined as a measure of strength of DNA binding and were significantly increased over that of the parent **6**, a result which suggests that the bisanthrapyrazoles **2**–**5** formed bisintercalation complexes with DNA. The concentration dependence of ΔT_m for compounds **2**–**5** (Fig. 2A and B) indicated that these compounds formed mainly bisintercalation complexes with DNA. Our docking results predicted **1** to have too short a linker to form a bisintercalation complex. This was confirmed by the results in Figure 2B in which compound **1** and monomeric compound **6** had the same slope and thus both formed mono intercalation complexes. GOLDScores obtained from docking and the experimentally determined ΔT_m values both displayed broad maxima (Fig. 5) when the bisanthrapyrazoles had 2–5 methylene linkers. The theoretical maximum value of ΔT_m, obtained from the quadratic fit to the experimentally determined ΔT_m values, predicts that a bisanthrapyrazole with 3 methylene linkers was optimal for DNA binding. Compound **3** with 3 methylene linkers had an experimentally measured ΔT_m value of 14.1 °C. This value is close to the experimentally measured value of 16.4 °C for **2**, the bisanthrapyrazole with 2 methylene linkers that was experimentally observed to bind the strongest to DNA (Table 1). Thus, the calculated and experimental DNA-binding affinities were in good agreement when used to select a range of optimal methylene linker lengths for synthesis.

The bisanthrapyrazoles have a relatively large number of rotatable bonds (up to 20 for **5**) and thus are highly conformationally flexible molecules that can adopt large numbers of low energy configurations. This high degree of conformational flexibility makes it computationally difficult to obtain the best possible GOLDScore. This fact likely explains the lack of a smooth change in GOLDScore as the number of linker groups is varied (Fig. 5A). Again considering the size of the bisanthrapyrazoles and the large number of rotatable bonds, the docking produced chemically reasonable bisintercalation complexes as shown in Figure 4. This result was likely due, in part, to the high affinity that the anthrapyrazole rings have for the doxorubicin-binding sites in which the bisanthrapyrazoles intercalate, thus anchoring the two ends of the bisanthrapyrazoles. Overall these results suggest that docking bisintercalators into X-ray structures of DNA is a useful tool for designing bisintercalating compounds with high affinity to DNA. DNA base specificity in bisanthrapyrazole binding to DNA may be another factor that may contribute to GOLDScores lacking the power to accurately predict DNA

binding as measured by ΔT_m. The bisanthrapyrazoles were docked into a single X-ray structure (PDB ID: 1DA9) which does not have the set of base pairs which necessarily leads to optimum binding to DNA. The base pair specificity of the bisanthrapyrazoles for calf thymus DNA is unknown.

In comparison with the monomer parent compound **6** (AP9) the bisanthrapyrazoles significantly inhibited the growth of K562 cells (Table 1). Though the bisanthrapyrazoles differed significantly in their ability to bind to DNA, this difference was not reflected in their ability to inhibit the growth of K562 cells. In fact, IC_{50} values for growth inhibition for the series varied only 3-fold. It can be speculated that this 'leveling' of activity may have occurred due to intra- or extracellular hydrolysis of the esters, either enzymatically through the action of esterases or non-enzymatically. For example, the diester succinylcholine is rapidly hydrolyzed by plasma cholinesterases.[23] Thus, compounds **1**–**5** may act as prodrugs (due to hydrolysis of the ester linkages) to produce a concentration of monomer **6** in the cells higher than that produced by **6** itself which results in only a moderate increment in cell growth inhibition. Thus, it can be concluded that while the design goal of increasing strength of DNA binding through bisintercalation was achieved, the goal of increasing cell growth inhibitory effects was not, possibly due to hydrolysis of the ester linkages in the bisanthrapyrazoles.

Bisanthrapyrazole inhibition of topoisomerase IIα catalytic activity was determined as a logical extension of our previous work demonstrating that **6** and the other anthrapyrazoles were strong topoisomerase IIα inhibitors.[4] The fact that cell growth inhibition was not correlated with inhibition of topoisomerase IIα-mediated catalytic decatenation activity suggests that the catalytic inhibition of topoisomerase II was not the primary mechanism by which these compounds inhibited cell growth. The anthrapyrazoles losoxantrone and piroxantrone, which have advanced to clinical trials,[24] likely exert their cell growth inhibitory effects by acting as DNA topoisomerase II poisons.[12,13] While many drugs that target topoisomerase II are strong DNA intercalators,[14] it is not an absolute requirement. However, the bisanthrapyrazoles were not strong inducers of the formation of linear DNA through stabilization of a covalent topoisomerase IIα–DNA cleavable complex in the DNA cleavage assay. Several of the anthrapyrazoles previously studied[4] did induce formation of linear DNA. This result does not rule out that the bisanthrapyrazoles were topoisomerase II poisons because these agents may have self-limiting action via their binding to DNA, as has been shown for doxorubicin at higher concentrations.[25] In our previous study we were also not able to specifically evaluate whether the parent **6** was able to induce formation of linear DNA due to its fluorescence in the gel obscuring the linear DNA band. The small, but general cross resistance (Table 1) that the anthrapyrazoles showed with the K/VP.5 cell line with decreased levels of topoisomerase IIα and topoisomerase IIβ[20,21] is seemingly consistent with the idea that the bisanthrapyrazoles may act as topoisomerase II poisons. Cells with less topoisomerase II in the cell produce fewer DNA strand breaks and because of this topoisomerase II poisons are less lethal to these cells.[14] The fact that a high level of cross resistance was not seen may be due to the fact that the bisanthrapyrazoles also target other DNA-processing enzymes due to their ability to intercalate into DNA.

In summary, a series of bisanthrapyrazoles were designed to bisintercalate into DNA using molecular modeling and docking. As predicted from the docking results, bisanthrapyrazoles with more than one methylene linker formed bisintercalation complexes with DNA and were significant inhibitors of K562 cell growth. Studies are in progress to produce bisanthrapyrazoles without potentially labile ester linkages.

4. Experimental

4.1. Biological assays

4.1.1. Materials. pBR322 plasmid DNA was obtained from MBI Fermentas (Burlington, Canada) and the kinetoplast plasmid DNA (kDNA) from TopoGEN (Columbus, OH). HindIII was from Invitrogen (Burlington, Canada). Unless indicated, other chemicals were from Sigma–Aldrich (Oakville, Canada). The 3-(4,5-dimethylthiazol-2-yl)-5-(3-carboxymethoxyphenyl)-2-(4-sulfophenyl)-2H-tetrazolium (MTS) CellTiter 96® AQueous One Solution Cell Proliferation Assay kit was obtained from Promega (San Luis Obispo, CA). Statistical analysis was done with SigmaStat (Systat, Point Richmond, CA).

4.1.2. Cell culture and growth inhibition assays. Human leukemia K562 cells, obtained from the American Type Culture Collection and K/VP.5 cells (a 26-fold etoposide-resistant K562-derived sub-line with decreased levels of topoisomerase IIα mRNA and protein)[18] were maintained as suspension cultures in DMEM (Dulbecco's modified Eagle's medium, Invitrogen, Burlington, Canada) containing 10% fetal calf serum (FCS) and 2 mM L-glutamine. The spectrophotometric 96-well plate cell growth inhibition MTS assay, which measures the ability of the cells to enzymatically reduce MTS after drug treatment, has been described.[4] The drugs were dissolved in DMSO. The final concentration of DMSO did not exceed 0.5% (v/v) and was an amount that had no detectable effect on cell growth. The cells were incubated with the drugs for the times indicated and then assayed with MTS. IC_{50} values for growth inhibition in both assays were measured by fitting the absorbance-drug concentration data to a four-parameter logistic equation as described.[4]

4.1.3. Topoisomerase IIα kDNA decatenation inhibition assay. A spectrofluorometric decatenation assay was used to determine the inhibition of topoisomerase IIα by the bisanthrapyrazoles.[4,19] kDNA consists of highly catenated networks of circular DNA. Topoisomerase IIα decatenates kDNA in an ATP-dependent reaction to yield individual minicircles of DNA. The 20 μL reaction

mixture contained 0.5 mM ATP, 50 mM Tris–HCl (pH 8.0), 120 mM KCl, 10 mM $MgCl_2$, 30 μg/mL bovine serum albumin, 50 ng kDNA, test compound (0.5 μL in DMSO), and 20 ng of topoisomerase IIα protein (the amount that gave approximately 80% decatenation). Using a high copy yeast expression vector, full-length human topoisomerase IIα was expressed, extracted, and purified as described previously.[19] The final DMSO concentration of 2.5% (v/v) was shown in controls not to affect the activity of topoisomerase IIα. The assay incubation was carried out at 37 °C for 20 min and was terminated by the addition of 12 μL of 250 mM Na_2EDTA. Samples were centrifuged at 8000*g* at 25 °C for 15 min and 20 μL of the supernatant was added to 180 μL of 600-fold diluted PicoGreen dye (Molecular Probes, Eugene, OR) in a 96-well plate. The fluorescence, which was proportional to the amount of kDNA, was measured in a Fluostar Galaxy (BMG, Durham, NC) fluorescence plate reader using an excitation wavelength of 485 nm and an emission wavelength of 520 nm.

4.1.4. pBR322 DNA relaxation and cleavage assays. Topoisomerase II-cleaved DNA complexes produced by anticancer drugs may be trapped by rapidly denaturing the complexed enzyme with sodium dodecyl sulfate (SDS).[4,16] The drug-induced cleavage of double-stranded closed circular pBR322 DNA to form linear DNA was followed by separating the SDS-treated reaction products using ethidium bromide gel electrophoresis as described.[16] The 20 μL cleavage assay reaction mixture contained 50 μM of the drug (0.5 μL in DMSO), 150 ng of topoisomerase IIα protein, 80 ng pBR322 plasmid DNA (MBI Fermentas, Burlington, Canada), 0.5 mM ATP in assay buffer (10 mM Tris–HCl, 50 mM KCl, 50 mM NaCl, 0.1 mM EDTA, 5 mM $MgCl_2$, 2.5% (v/v) glycerol, pH 8.0. The order of addition was assay buffer, DNA, drug, and then topoisomerase IIα. The reaction mixture was incubated at 37 °C for 10 min and quenched with 1% (v/v) SDS/25 mM Na_2EDTA. The reaction mixture was treated with 0.25 mg/mL proteinase K (Sigma) at 55 °C for 30 min to digest the protein. The linear pBR322 DNA cleaved by topoisomerase IIα was separated by electrophoresis (2 h at 8 V/cm) on a TAE (Tris base (4 mM)/glacial acetic acid (0.11% (v/v))/Na_2EDTA (2 mM) buffer)/ethidium bromide (0.5 μg/mL)/agarose gel (1.2%, wt/v)). Ethidium bromide was used in the gel and running buffer in order that the inhibition of relaxation activity could be measured along with formation of cleaved linear DNA. The DNA in the gel was imaged by its fluorescence on a Alpha Innotech (San Leandro, CA) Fluorochem 8900 imaging system equipped with a 365 nm UV illuminator and a CCD camera.

4.1.5. Thermal denaturation of DNA assay. Compounds that intercalate into DNA stabilize the DNA double helix and increase the temperature at which the DNA is denatured or unwinds.[8,10,26] The effect of 2 μM of the bisanthrapyrazoles on the DNA thermal melt temperature (ΔT_m) of sonicated calf thymus DNA (5 μg/mL) was measured in 10 mM Tris–HCl buffer (pH 7.5) in a Cary 1 (Varian, Mississauga, Canada) double beam spectrophotometer by measuring the absorbance increase at 260 nm upon the application of a temperature ramp of 1 °C/min. The maximum of the first derivative of the absorbance-temperature curve was used to obtain the ΔT_m as we previously described.[4] Doxorubicin (2 μM), which is a strong DNA intercalator, was used as a positive control.[4,8] In order to determine whether the bisanthrapyrazoles formed bisintercalation complexes with DNA the concentration dependence of ΔT_m was measured from 0.1 to 2 μM anthrapyrazole or bisanthrapyrazole as described above in 10 mM Tris–HCl buffer (pH 8.0) at a DNA concentration of 20 μM (base pair basis). The slopes of the plots for monomer **6** were compared with that of the bisanthrapyrazoles **1**–**5** using a *t*-test comparison of the slopes.[27]

4.2. Molecular modeling and docking

4.2.1. Docking of the bisanthrapyrazoles into an X-ray structure of DNA. All molecular modeling was done using SYBYL 7.3[28] on a Hewlett-Packard XW4100 PC workstation with a Redhat Enterprise 4 Linux operating system. All molecules except the DNA were built using SYBYL. Compound **6** and the bisanthrapyrazoles were docked into the doxorubicin-binding site of a 6-base pair X-ray crystal structure of 2 molecules of doxorubicin bound to double-stranded DNA, d(TGGCCA)/doxorubicin, (http://www.rcsb.org/pdb/ PDB ID: 1DA9)[22] using the genetic algorithm docking program GOLD version 3.1[29] with default GOLD parameters and atom types and with 100 starting runs.[30] GOLDScore was used as the fitness function with flipping options of planar and pyramidal nitrogens being allowed. Internal ligand energy offset was set to on. No early termination was allowed.

The 1DA9 X-ray structure shows that the first and second base pairs buckle out to accommodate the bound doxorubicin.[22] Thus, the 1DA9 X-ray structure of the doxorubicin–DNA complex was used for the docking experiments, rather than constructing DNA in SYBYL because it was reasoned that this DNA structure would be a more realistic model for binding of bisanthrapyrazoles. Additionally, the bisanthrapyrazoles are structurally similar to doxorubicin (Fig. 1). In the 1DA9 X-ray structure the two doxorubicin molecules are separated by four intervening base pairs. This structure was chosen because it was reasoned that DNA molecules with a smaller number of intervening base pairs would have to distort the DNA double helix (with an accompanying energy penalty) in order to bind. The protonated bisanthrapyrazoles were first geometry optimized with the Tripos force field using a conjugate gradient with a convergence criterion of 0.01 kcal/mol and Gasteiger–Huckel charges and a distance-dependent dielectric constant. The DNA structure was prepared by removing both of the bound doxorubicin molecules and removing all water molecules to avoid potential interference with the docking. Hydrogens were added to the DNA with the SYBYL Biopolymer module. The binding site was defined using an atom in the center of the DNA molecule and was large enough that it encompassed both of the doxorubicin-binding sites. Initial docking runs showed that not all bisanthrapyrazoles docked with the linker lo-

cated in the DNA minor groove. Thus, docking runs were also carried out with the major groove blocked with a small molecule in order to compare all bisanthrapyrazoles docked into the minor groove. The bisanthrapyrazoles ($n = 0$–9) were docked into the DNA structure to obtain the top 10 scoring GOLDScore structures for each molecule and their individual component energy terms. The top structures were then rescored using a local optimization (simplexing) to obtain the final GOLDScore. Rescoring did not affect the initial relative scoring order. As a test of the docking procedure doxorubicin was docked back into the DNA structure with a heavy atom root-mean-squared distance of 1.3 Å compared to the X-ray structure.[22] Values of 2.0 Å or less in the extensive GOLD test set are considered to be good.[30] The graphic in Figure 4 was prepared with DS Visualizer 1.7 (Accelrys, San Diego, CA).

4.3. Chemistry

4.3.1. General. Melting points were taken on a Gallenkamp (Loughborough, England) melting point apparatus and are uncorrected. Electrospray ionization mass spectra (ESI-MS) were acquired on an Applied Biosystems API 2000 Triple Quadrupole mass spectrometer (Thornhill, Toronto, Canada) equipped with a syringe pump. Samples (~1 mM in acetonitrile) were injected into the ion source at a flow rate of 5 μL/min. ^{1}H and ^{13}C nuclear magnetic resonance (NMR) spectra were recorded at 300 K in 5 mm NMR tubes on a Bruker Avance 500 spectrometer operating at 500.14 MHz for ^{1}H NMR and 125.8 MHz for ^{13}C NMR, respectively, on solutions in dimethyl sulfoxide-d_6 (DMSO-d_6), unless otherwise indicated. Chemical shifts are given in parts per million (ppm) (±0.01 ppm) relative to that of tetramethylsilane (TMS) (0.00 ppm) in the case of the ^{1}H NMR spectra, and to the central line of DMSO-d_6 (δ 39.5) for the ^{13}C NMR spectra. The ^{1}H NMR spectrum of **4** was run on a Varian Mercury 300 MHz NMR. TLC was performed on aluminum-backed plates bearing 200 μm silica gel 60 F_{254} (Silicycle, Quebec City, Canada). Compounds were visualized by quenching of fluorescence by UV light (254 nm) where applicable. The reaction conditions were not optimized for reaction yields. Dichloromethane and triethylamine were refluxed with calcium hydride and distilled. Compound **6** (7-chloro-2-[2-[(2-hydroxyethyl)methylamino]ethyl]anthra[1,9-**cd**]pyrazol-6(2H)-one) was prepared from 1,5-dichloroanthraquinone as we previously described.[4]

4.3.2. General procedure for the synthesis of the bisanthrapyrazoles. A solution of the acid chloride (0.5 equiv, 0.2 M) in dichloromethane was added to a clear orange-red solution of **6** and triethylamine (8 equiv) in dichloromethane (3 mL). Yellow precipitates separated after 20 min. The reaction mixture was stirred at room temperature overnight, diluted with diethyl ether (10 mL), and filtered. The yellow solid obtained was washed with dichloromethane (3× 5 mL) and dried in vacuum.

4.3.2.1. Bis(2-((2-(7-chloro-6-oxo-6H-dibenzo[*cd*,*g*]indazol-2-yl)-ethyl)-methyl-amino)-ethyl) malonate (1). Compound **6** (53.2 mg, 0.149 mol) reacted with malonyl chloride (0.37 mL, 0.075 mmol) affording **1** as a yellow solid. Yield 25.5 mg (21.5%); mp: 138.0–141.0 °C; ^{1}H NMR δ 8.25–7.55 (m, 12H, ArH), 5.13 (m, 4H, 2× $NNCH_2$), 4.50 (m, 4H, 4× OCH_2), 3.90–3.40 (m, 8H), 3.45 (s, 2H, $COCH_2CO$), 2.92 (s, 6H, 2× NCH_3); ^{13}C NMR δ 182.6, 182.3, 169.5, 168.9, 167.7, 167.1 (6× CO), 140.2, 140.1, 139.1, 138.9, 137.0, 137.0, 135.2, 135.1, 135.0, 134.9, 133.9, 133.8, 130.4, 130.2, 129.5, 129.4, 127.1, 126.9, 123.2, 123.1, 123.1, 123.0, 1221.1, 122.0, 117.8, 117.7 (ArC), 60.3, 60.1 (2× OCH_2), 56.1, 55.2, 55.0, 54.8, 45.3, 43.1, 42.6, 42.2, 41.4 ($COCH_2CO$); MS (ESI *m*/*z*): calcd for $[C_{41}H_{36}Cl_2N_6O_6+H]^+$ 779.2, found 779.3.

4.3.2.2. Bis(2-((2-(7-chloro-6-oxo-6H-dibenzo[*cd*,*g*]indazol-2-yl)-ethyl)-methyl-amino)-ethyl) succinate (2). Compound **6** (48.1 mg, 0.135 mmol) reacted with succinyl chloride (0.34 mL, 0.068 mmol) affording **2** as a yellow solid. Yield 41.7 mg (38.8%); mp: 180 °C (decomposed); ^{1}H NMR δ 8.24–7.57 (m, 12H, ArH), 5.11 (br s, 4H, 2× $NNCH_2$), 4.44 (br s, 4H, 2× OCH_2), 3.86–3.45 (m, 8H), 2.92 (s, 6H, 2× NCH_3), 2.64 (br s, 4H, $COCH_2CH_2CO$); ^{13}C NMR δ 181.8, 181.6, 171.9 (CO), 139.3, 138.2, 136.2, 134.4, 134.3, 134.1, 133.0, 129.4, 128.6, 126.2, 122.3, 121.1, 116.9 (ArC), 57.7 (OCH_2), 55.5, 54.8, 54.2, 44.4 (NCH_3), 29.0 ($COCH_2CH_2CO$). MS (ESI *m*/*z*): calcd for $[C_{42}H_{38}Cl_2N_6O_6+H]^+$ 793.2, found 793.3.

4.3.2.3. Bis(2-((2-(7-chloro-6-oxo-6H-dibenzo[*cd*,*g*]indazol-2-yl)-ethyl)-methyl-amino)-ethyl) glutarate (3). Compound **6** (81.9 mg, 0.230 mol) reacted with glutaryl chloride (0.58 mL, 0.115 mmol) affording **3** as a yellow solid. Yield 104.5 mg (57.2%); mp: 111.5–113.0 °C;^{1}H NMR δ 8.03–7.12 (m, 12H, ArH), 4.92 (s, 4H, 2× $NNCH_2$), 4.25 (4H, 2× OCH_2), 3.63, 3.55, 3.42, 3.31 (4s, 8H), 2.73 (s, 6H, 2× NCH_3), 2.23, 2.01 (2s, 4H, 2× $COCH_2$), 1.60 (m, 2H, $COCH_2CH_2$); ^{13}C NMR δ 181.6, 181.4, 1774.3, 172.5 (CO), 139.4, 139.1, 138.2, 138.1, 136.1, 136.0, 134.3, 134.3, 134.2, 134.1, 133.0, 129.5, 129.4, 128.6, 128.4, 126.2, 126.0, 122.3, 122.3, 122.2, 122.1, 121.2, 121.1, 116.9, 116.7 (ArC), 58.5 (OCH_2), 54.2 (NCH_2), 44.4 (NCH_3), 32.9, 20.8 ($COCH_2CH_2CH_2CO$); MS (ESI *m*/*z*): calcd for $[C_{43}H_{40}Cl_2N_6O_6+H]^+$ 807.2, found 807.4.

4.3.2.4. Bis(2-((2-(7-chloro-6-oxo-6H-dibenzo[*cd*,*g*]indazol-2-yl)-ethyl)-methyl-amino)-ethyl) adipate dihydrochloride (4). Compound **6** (106 mg, 0.30 mmol) in $CHCl_3$ (2.5 mL) was treated at 0 °C with adipoyl chloride (0.75 mL of a 0.2 M solution in $CHCl_3$) and the mixture allowed to come to room temperature while stirring overnight. Within 1 h a yellow precipitate began to form. At 18 h the mixture was diluted with ether (10 mL) and centrifuged. The resulting yellow crystals were dried in a nitrogen stream and then under vacuum overnight affording the dihydrochloride of **4**. The sample was recrystallized from methanol-ether affording yellow crystals. Yield: 70 mg (53%), ^{1}H NMR δ 8.24–7.60 (m, 12H, ArH), 5.05 (s, 4H, 2× $NNCH_2$), 4.35 (br s, 4H, 2× OCH_2), 3.80 (br s, 4H), 2.90 (s, 6H, 2× NCH_3), 2.20 (br s, 4H, 2× $COCH_2$), 1.25 (br s, 2H, $COCH_2CH_2$), MS (ESI *m*/*z*): calcd for $[C_{44}H_{42}Cl_2N_6O_6+H]^+$ 821.3, found 821.4.

4.3.2.5. Bis(2-((2-(7-chloro-6-oxo-6H-dibenzo[*cd*,*g*]indazol-2-yl)-ethyl)-methyl-amino)-ethyl) pimelate (5). Compound **6** (51.5 mg, 0.145 mol) reacted with pimeloyl chloride (0.36 mL, 0.115 mmol) affording **5** as a yellow solid. Yield 64.5 mg (56.1%); mp: 102.0–104.0 °C; ^{1}H NMR δ 8.26–7.57 (m, 12H, ArH), 5.18 (s, 4H, 2× $NNCH_2$), 4.48 (s, 4H, 2× OCH_2), 3.89, 3.81, 3.67, 3.56 (4s, 8H), 2.99 (s, 6H, 2× NCH_3), 2.34 (t, J = 7.3 Hz, 4H, 2× $COCH_2$), 1.50 (m, 4H, 2× $COCH_2CH_2$), 1.24 (m, 2H, $COCH_2CH_2CH_2$); ^{13}C NMR δ 181.4, 174.7, 172.7 (CO), 139.2, 138.1, 136.1, 134.2, 134.1, 133.0, 129.4, 128.5, 126.0, 122.2, 122.1, 121.1, 116.9 (ArC), 58.5 (OCH_2), 54.1 (NCH_2), 44.4 (NCH_3), 33.5, 28.1, 24.1 ($COCH_2CH_2CH_2$); MS (ESI *m*/*z*): calcd for $[C_{45}H_{44}Cl_2N_6O_6+H]^+$ 835.3, found 835.3.

Acknowledgments

Supported by grants from the Canadian Institutes of Health Research, the Canada Research Chairs Program, a Canada Research Chair in Drug Development to Brian Hasinoff, the Robert A. Welch Foundation (Grant AF-0005) the Herbert and Kate Dishman Endowment at Southwestern University to Frank Guziec and an NIH (Grant CA90787) to Jack Yalowich.

References and notes

1. Hartley, J. A.; Reszka, K.; Zuo, E. T.; Wilson, W. D.; Morgan, A. R.; Lown, J. W. *Mol. Pharmacol.* **1988**, *33*, 265–271.
2. Showalter, H. D.; Johnson, J. L.; Hoftiezer, J. M.; Turner, W. R.; Werbel, L. M.; Leopold, W. R.; Shillis, J. L.; Jackson, R. C.; Elslager, E. F. *J. Med. Chem.* **1987**, *30*, 121–131.
3. Fry, D. W.; Boritzki, T. J.; Besserer, J. A.; Jackson, R. C. *Biochem. Pharmacol.* **1985**, *34*, 3499–3508.
4. Liang, H.; Wu, X.; Guziec, L. J.; Guziec, F. S. J.; Larson, K. K.; Lang, J.; Yalowich, J. C.; Hasinoff, B. B. *J. Chem. Inf. Model.* **2006**, *46*, 1827–1835.
5. Dawson, S.; Malkinson, J. P.; Paumier, D.; Searcey, M. *Nat. Prod. Rep.* **2007**, *24*, 109–126.
6. Martinez, R.; Chacon-Garcia, L. *Curr. Med. Chem.* **2005**, *12*, 127–151.
7. Portugal, J.; Cashman, D. J.; Trent, J. O.; Ferrer-Miralles, N.; Przewloka, T.; Fokt, I.; Priebe, W.; Chaires, J. B. *J. Med. Chem.* **2005**, *48*, 8209–8219.
8. Priebe, W.; Fokt, I.; Przewloka, T.; Chaires, J. B.; Portugal, J.; Trent, J. O. *Methods Enzymol.* **2001**, *340*, 529–555.
9. Malisza, K. L.; Hasinoff, B. B. *Arch. Biochem. Biophys.* **1995**, *321*, 51–60.
10. McGhee, J. D. *Biopolymers* **1976**, *15*, 1345–1375.
11. Bjorndal, M. T.; Fygenson, D. K. *Biopolymers* **2002**, *65*, 40–44.
12. Leteurtre, F.; Kohlhagen, G.; Paul, K. D.; Pommier, Y. *J. Nat. Cancer Inst.* **1994**, *86*, 1239–1244.
13. Capranico, G.; Palumbo, M.; Tinelli, S.; Mabilia, M.; Pozzan, A.; Zunino, F. *J. Mol. Biol.* **1994**, *28*, 1218–1230.
14. Fortune, J. M.; Osheroff, N. *Prog. Nucleic Acid Res. Mol. Biol.* **2000**, *64*, 221–253.
15. Li, T. K.; Liu, L. F. *Annu. Rev. Pharmacol. Toxicol.* **2001**, *41*, 53–77.
16. Burden, D. A.; Froelich-Ammon, S. J.; Osheroff, N. *Methods Mol. Biol.* **2001**, *95*, 283–289.
17. Hasinoff, B. B.; Wu, X.; Begleiter, A.; Guziec, L.; Guziec, F.; Giorgianni, A.; Yang, S.; Jiang, Y.; Yalowich, J. C. *Cancer Chemother. Pharmacol.* **2006**, *57*, 221–233.
18. Fattman, C.; Allan, W. P.; Hasinoff, B. B.; Yalowich, J. C. *Biochem. Pharmacol.* **1996**, *52*, 635–642.
19. Hasinoff, B. B.; Wu, X.; Krokhin, O. V.; Ens, W.; Standing, K. G.; Nitiss, J. L.; Sivaram, T.; Giorgianni, A.; Yang, S.; Jiang, Y.; Yalowich, J. C. *Mol. Pharmacol.* **2005**, *67*, 937–947.
20. Ritke, M. K.; Allan, W. P.; Fattman, C.; Gunduz, N. N.; Yalowich, J. C. *Mol. Pharmacol.* **1994**, *46*, 58–66.
21. Ritke, M. K.; Roberts, D.; Allan, W. P.; Raymond, J.; Bergoltz, V. V.; Yalowich, J. C. *Br. J. Cancer* **1994**, *69*, 687–697.
22. Leonard, G. A.; Hambley, T. W.; McAuley-Hecht, K.; Brown, T.; Hunter, W. N. *Acta Crystallogr. D Biol. Crystallogr.* **1993**, *49*, 458–467.
23. Testa, B.; Mayer, J. M. *Hydrolysis in Drug and Prodrug Metabolism: Chemistry Biochemistry and Enzymology*; Wiley-VCH: Zèurich, Weinheim, 2003, pp 396–398.
24. Gogas, H.; Mansi, J. L. *Cancer Treat. Rev.* **1996**, *21*, 541–552.
25. Tewey, K. M.; Rowe, T. C.; Yang, L.; Halligan, B. D.; Liu, L. F. *Science* **1984**, *226*, 466–468.
26. Sissi, C.; Leo, E.; Moro, S.; Capranico, G.; Mancia, A.; Menta, E.; Krapcho, A. P.; Palumbo, M. *Biochem. Pharmacol.* **2004**, *67*, 631–642.
27. Jones, D. *Pharmaceutical Statistics*; Pharmaceutical Press: London, 2002, p 585.
28. SYBYL 7.3, Tripos Inc., 1699 South Hanley Rd., St. Louis, MO, 63144, USA.
29. GOLD 3.1, CCDC Software Ltd, Cambridge, UK.
30. Verdonk, M. L.; Cole, J. C.; Hartshorn, M. J.; Murray, C. W.; Taylor, R. D. *Proteins* **2003**, *52*, 609–623.